

Far- and near-field optical properties of gold nanoparticle ensembles*

N.N. Nedyalkov, A. Dikovska, I. Dimitrov, Ru. Nikov, P.A. Atanasov, R.A. Toshkova, E.G. Gardeva, L.S. Yossifova, M.T. Alexandrov

Abstract. The optical properties of gold nanoparticle clusters are presented from the point of view of their applications in biophotonics, where the absorption and scattering spectra are crucial. Generalised multiparticle Mie theory and finite difference time domain (FDTD) technique are used for theoretical description of the far- and near-field optical properties of two dimensional nanoparticle ensembles. The system under consideration consists of spherical gold nanoparticles from 20 to 200 nm in diameter, forming 2D clusters in water. The properties of the far-field absorption and scattering spectra as a function of the cluster size, particle dimensions, and interparticle distance are investigated for ordered hexagonal structure of the particle arrays. It is found that the absorption efficiency can be shifted to the IR spectral range by increasing array size and decreasing interparticle distance. The increase in the array size also results in enhancement of the scattering efficiency while the absorption is reduced. The near-field intensity distribution is inhomogeneous over the array, as formation of zones with intensity enhancement of about two orders of magnitude is observed in specific areas. The optical properties of an ensemble whose configuration is reproduced from real experiments of gold nanoparticle deposition onto cancer cells are also presented. The results obtained can be used in designing of nanoparticle arrays with applications in biophotonics, bioimaging and photothermal therapy.

Keywords: gold nanoparticle ensembles, optical properties, plasmon excitation.

1. Introduction

Recent progress in fabrication and manipulation of nanoparticles accelerates the research activities in development of reliable description of their unique properties and designing new applications [1]. Most of these applications relay on the specific properties of the interaction between nanoparticles and the electromagnetic field. For noble metal nanoparticles this interaction is related to the ability of efficient plasmon excita-

tion in these structures which drastically changes their optical properties [2, 3]. For these metals the resonance frequency is in the near-UV–VIS spectral range where commercially available laser systems work. Under resonance conditions the absorption and scattering coefficients are strongly enhanced and the values can be more than several orders of magnitude higher compared to organic dyes used in photothermal and photodynamic therapy [4]. The plasmon excitation also results in specific properties of the electromagnetic field in the close vicinity of nanoparticles [5]. The field intensity can be strongly enhanced in so-called ‘hot spots’ that have characteristic size defined by the particle dimensions. Thus, the diffraction limit imposed on conventional optics can be overcome and light intensity localisation at dimensions smaller compared to the wavelength of the incident irradiation is possible.

The theoretical and experimental studies on the properties of noble metal nanoparticles [2, 3, 6] show that they can be efficiently modified since the plasmon resonance frequency depends on the size, shape, and orientation of the particle with respect to the polarisation of the incident irradiation, dielectric properties of the environment, geometry of the irradiation. These properties found applications in biological applications where noble metal nanoparticles are used in targeted drug delivery [7] and bioimaging [4]. The enhanced absorption of a nanoparticle under resonance conditions can also lead to its strong heating that will result in triggering of irreversible chemical effects, protein denaturation or bubble formation in the biomaterial in its vicinity. Since the size of cells and their organelles falls in the micron and submicron scale the application of nanoparticles can allow strong localisation of the processing area even within the cell. Furthermore, by changing such particle properties as shape, size, and structure, the resonance frequency can be shifted to the transparency window of the tissue [8, 9] and only area in close vicinity of the nanoparticle can be affected. The near-field intensity enhancement in the vicinity of nanoparticles is the basis of surface enhanced Raman spectroscopy (SERS) that is capable of detecting even a single molecule [10].

The unique properties of nanoparticles are even more exciting when 2 and 3-dimensional ensembles are considered [6, 11]. In such structures the optical spectra have a more complex structure that results from electromagnetic coupling of neighbouring particles [12–15]. When the interparticle distance is less than the particle diameter, near-field coupling is realised and the field intensity is strongly localised in the gap between particles. This effect also induces a shift of the resonance frequency with respect to the single particle case. For particles largely separated from each other, the far-field coupling is realised as it is influenced by the interference of the scattered light from neighbouring particles. In contrast to the single particle, the spectra of nanoparticle ensembles can be more

* Reported at the XIX International Conference on Advance Laser technologies (ALT’11), September 2011, Golden Sands, Bulgaria.

N.N. Nedyalkov, A. Dikovska, I. Dimitrov, Ru. Nikov, P.A. Atanasov
Institute of Electronics, Bulgarian Academy of Sciences, Tzarigradsko
shousse 72, Sofia 1784, Bulgaria; e-mail: nnn_1900@yahoo.com;
R.A. Toshkova, E.G. Gardeva, L.S. Yossifova, M.T. Alexandrov
Institute of Experimental Morphology, Pathology and Anthropology,
Bulgarian Academy of Sciences, G. Bonchev Street, bl. 25, Sofia 1113,
Bulgaria

Received 24 May 2012; revision received 18 July 2012
Kvantovaya Elektronika 42 (12) 1123–1127 (2012)
Submitted in English

efficiently modified and tuned by changing the interparticle distance and orientation of the array with respect to the polarisation of the incident irradiation. These properties are used in designing of active substrates in SERS applications and photothermal therapy of cancer cells [9, 15]. In the latter case it is found that using of nanoparticle aggregates significantly reduces the cancer cell killing threshold and a pronounced increase in the treatment efficiency is observed.

In this paper we focus our attention on the optical spectra of noble metal nanoparticle ensembles, and their dependences on different characteristics – particle size, interparticle distance, shape of the system. The distribution of the electromagnetic field in the vicinity of the arrays is also shown. Although these properties has been an object of interest for decades, the applications, especially in the field of biophotonics, still need a detailed description in terms of particular shape, size and environment of the nanoparticle systems. As an example we show optical properties of a nanoparticle system that is observed in cancer cells in experiments on photothermal therapy. In our analysis we also include near-field properties of a nanoparticle array which usually are not considered when it comes to their applications in biophotonics. The results of this study show some efficient parameters for optical properties manipulation and can be used in designing applications in biophotonics and SERS. In these applications the position of the plasmon resonance band and respectively the optimal absorption and scattering wavelengths are of crucial importance.

2. Theoretical model

The optical properties of 2D arrays are described in terms of normalised efficiencies ($Q_{\text{ext, sca, abs}}$) that are given by the extinction, scattering or absorption cross section divided by the geometrical cross section of the array. The cross sections are calculated on the basis of the GMM (generalised multiparticle Mie) approach [16]. The input data for the GMM code are the coordinates of the centre of each particle and its radius. The simulated system assumed in this study consists of gold nanoparticle arrays with particles having a diameter of 20, 40 or 100 nm in water. This system is used to mimic the real case of gold nanoparticle in biomaterial environment, since water makes up a significant portion of most soft tissues and is often used as convenient modelling system [17]. The incident radiation is not polarised and its wave vector is directed perpendicularly to the nanoparticle array plane.

The FDTD simulation model is applied to study the near-field properties around the irradiated nanoparticles. This computational technique, based on the numerical solution of Maxwell's equations [18] is proven to give an adequate picture of the electromagnetic field distribution in the near- and far-fields around structures with arbitrary shapes [19]. In the simulations a plane wave irradiates gold particles. The electric field strength of the incident irradiation is set at 1 V m^{-1} . The optical properties (dielectric function) of the investigated substrate materials are introduced in the model by using data taken from Refs [20, 21]. All calculations are performed with the assumption that the surrounding medium is water at 20°C and the wavelength-independent refractive index n_{med} is taken equal to 1.333.

3. Results and discussion

The analysis of the optical properties of nanoparticle systems is focused on the influence of the array size (number of particles),

particle dimensions, interparticle distance, and the shape of the array. The studied system has a hexagonal arrangement of the particles since this structure is usually obtained in self-assembly deposition. Figure 1 shows the absorption spectra of gold nanoparticle arrays composed of different number of particles with a diameter of 20, 40, and 100 nm. The spectra for a single particle are also presented. The increase in the particle number results in a widening of the absorption band for all particle diameters. The enlargement of the array size also results in a shift of the absorption peaks to longer wavelengths as their intensity decreases. For a system composed of particles with a diameter of 20 nm, the absorption efficiency value exceeds the single particle one for arrays with size up to 4×4 . For the larger structures (8×8 and 10×10) the peak

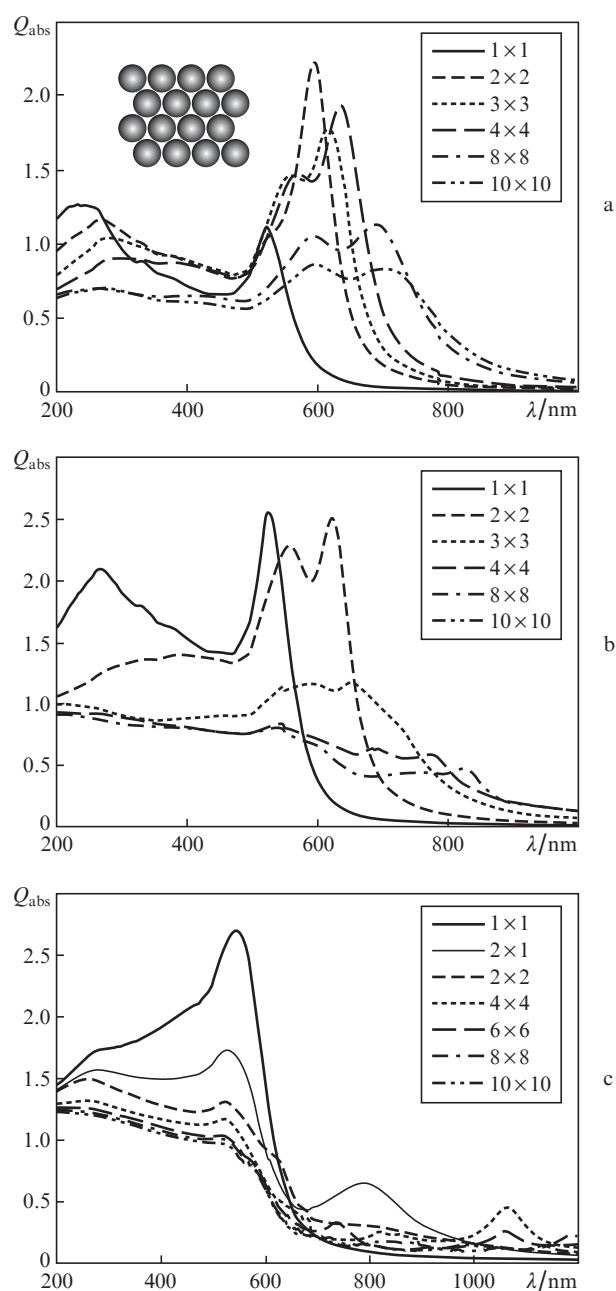


Figure 1. Absorption efficiency spectra of gold nanoparticle arrays composed of different number of particles with a diameter of (a) 20, (b) 40, and (c) 100 nm. The spectra for a single particle are also presented.

intensity is comparable to the single particle case; however, the absorption band wing is expanded into IR region to wavelength of about 1000 nm. The arrays composed of nanoparticles with larger diameters demonstrate a well pronounced decrease in the absorption efficiency which is lower than the single particle case even at size of 2×2 particles. For systems composed of 40-nm particles a pronounced absorption efficiency is observed in the spectral range between 800 and 1000 nm and its peak values at 8×8 and 10×10 are maximal compared to the case of 20- and 100-nm particle systems. In the case of a 100-nm particle size, the single particle ensures the maximal absorption efficiency, as it rapidly decreases with increasing particle number in the array. For 4×4 and 6×6 systems the peaks in absorption efficiency are observed at 1050 nm.

For multiparticle systems the optical spectra consist of peaks related to excitation of different plasmon modes in a single particle within the array as well as to collective excitations. Figure 2 shows the absorption efficiency spectra of two nanoparticle chains composed of 4 and 9 touching gold nanoparticles with a diameter of 20 nm. This structure exhibits two main maxima in the absorption spectrum. The short-wavelength maximum corresponds to plasmon resonance of particles excited by the electric field component perpendicular to the chain long axis. The position of this maximum does not depend on the length of the chain, and it shows a weak dependence on the particle size. The long-wavelength maximum is related to plasmon excitation along the nanoparticle chain. Its resonance position is strongly dependent on the chain length. Our simulations show that the long-wavelength maxima in the absorption spectra are red shifted and the absorption efficiency increases with increasing particle number within the chain. Compared to the other arrays, this structure offers more efficient tuning of the resonance wavelength by changing the number of nanoparticles.

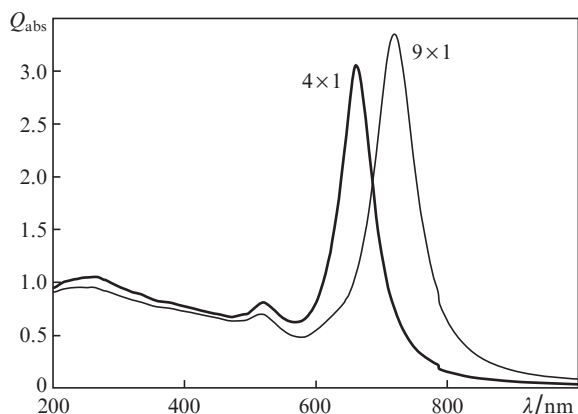


Figure 2. Absorption efficiency spectra of nanoparticle chains composed of 4 and 9 gold nanoparticles 20 nm in diameter.

Another parameter that influences the optical properties of nanoparticle arrays is interparticle distance. Due to the evanescent nature of the near electromagnetic field, the near-field coupling between neighbouring particles is realised only at distances in the range of particle dimensions. Figure 3 represents the absorption efficiency spectra of 4×4 nanoparticle arrays with a particle diameter of 40 nm for different interparticle distances. In all cases the maximal value is lower compared to the case of a single particle. With an increase in the interparticle distance the plasmon band shifts to the shorter

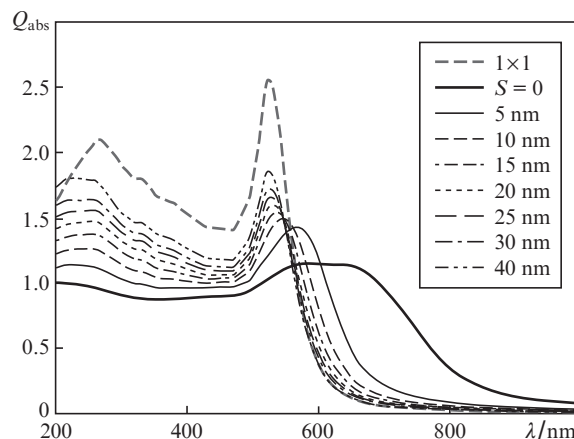


Figure 3. Absorption efficiency spectra of 4×4 nanoparticle arrays with particles 40 nm in diameter for different interparticle distances.

wavelengths as at distances larger than 30 nm the position of the maximum coincides with that of an isolated particle.

The absorption spectra discussed up to now can be a basis for designing optimal conditions for photothermal therapy based on laser heating of gold nanoparticles. In other applications, for example bioimaging, the scattering properties are most important. For a single particle case at small particle size, where phase retardation and excitation of higher multipoles are negligible, the optical response is dominated by dipole absorption [2]. With an increase in the particle dimensions the contribution of scattering increases and at sizes above few tens of nanometers it dominates the optical spectra and gives the main contribution to the overall extinction. A similar effect is observed also for nanoparticle ensembles with different size. An example is shown in Fig. 4 where optical properties of two nanoparticle arrays composed of 2×2 and 4×4 nanoparticles with diameters of 40 nm are presented. For a smaller structure the magnitude of the absorption maximum at 620 nm exceeds the scattering one by more than 2 times. For a bigger array the scattering dominates over the absorption as the maximum in the scattering spectra is red shifted with respect to absorption.

Recent studies of the interaction of the electromagnetic field and noble metal nanoparticles show [5, 22] that the near-field intensity in the particle vicinity can be efficiently enhanced to values that may induce even a permanent modification in the neighbouring medium. This effect may be important in biophotonic applications where nanoparticles can be deposited on a cell membrane or enter the cells and due to field enhancement to induce or accelerate different photo- and biochemical reactions. Figure 5 shows the distribution of the electric field intensity in the vicinity of a nanoparticle array composed of particles with diameters of 100 nm. The incident irradiation is assumed to be a circularly polarised plane wave at $\lambda = 532$ nm. The near-field intensity distributions in a plane under the array and in a plane through a chain from the array are presented. It is seen that the field intensity is strongly enhanced in zones located in the gaps between the particles. There the intensity is about two orders of magnitude higher compared to the incident one. Under the arrays the enhancement is lower (about 5).

The near-field properties on a nanoparticle array depend on the environmental dielectric properties. In the vicinity of the contact point the near-field intensity distribution is governed by the interaction with the image charges induced in the envi-

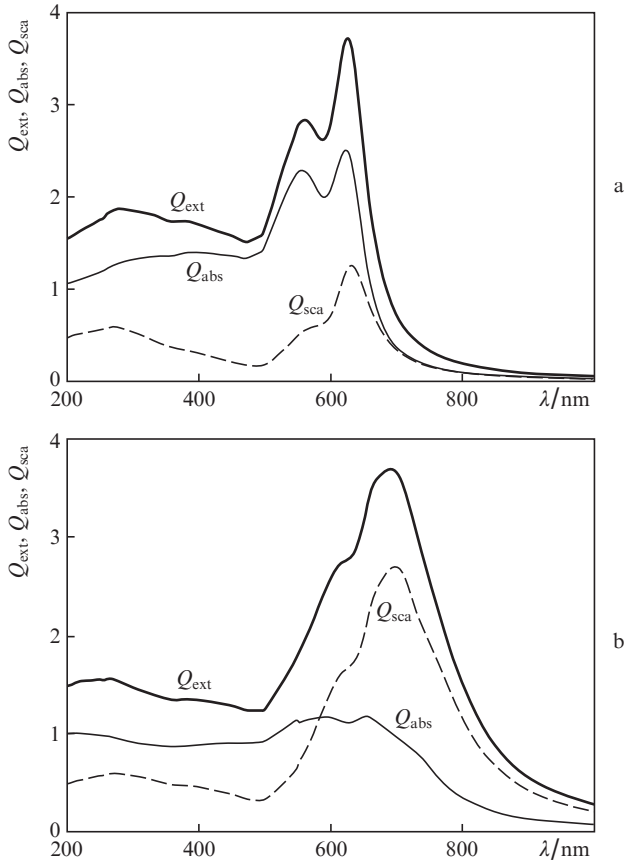


Figure 4. Extinction, absorption and scattering efficiency spectra of nanoparticle arrays composed of 2×2 and 4×4 nanoparticles 40 nm in diameter.

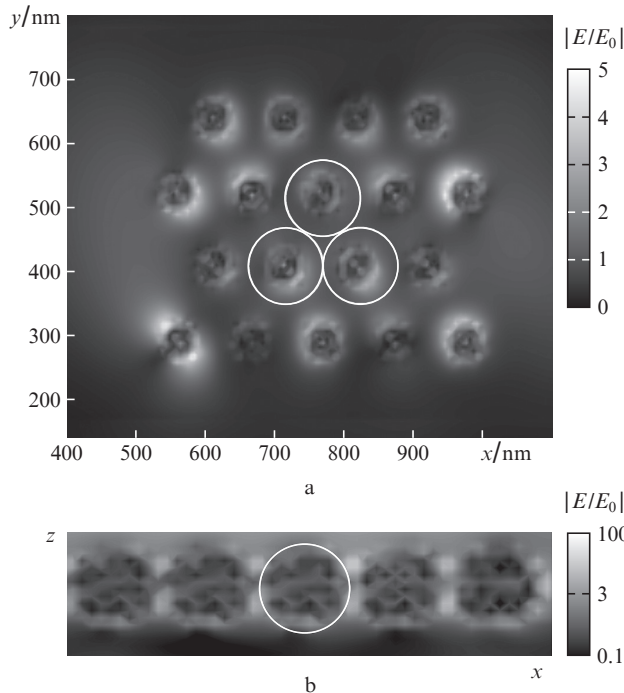


Figure 5. FDTD results of the distribution of the electric field intensity E in the vicinity of nanoparticle array composed of 18 particles 100 nm in diameter. The incident irradiation is assumed to be a circularly polarised plane wave at $\lambda = 532$ nm. The near-field intensity distributions in a plane under the array and in a plane through a chain from the array are presented. The white circles represent delineation of some particles.

ronment. A study in this direction could be related to application of nanoparticles in sensing and processing. Figure 6 shows the results of FDTD simulation in a complex geometry. The system under consideration here consists of 100-nm Au nanoparticles deposited on a dielectric substrate with a dielectric constant ϵ_s . On the top of the array is deposited a dielectric material with a dielectric constant ϵ_m . The distribution of the electric field intensity is shown for two cases: $\epsilon_s > \epsilon_m = \epsilon_s/2$ and $\epsilon_s < \epsilon_m = 2\epsilon_s$. It is seen that in the first case the zones with the maximal intensity are localised in the vicinity of the contact points of the particles with the substrate. In this case the maximal value of the intensity is about two times higher compared to that in contact points of the particles and the material deposited on the top. When the material on the top of the array has a higher value of the dielectric constant than the substrate, the hot spots are located on the top of the array. This localisation is important since it is shown that the near-field intensity enhancement at these points can induce permanent modification of material located in close vicinity of the particles [5].

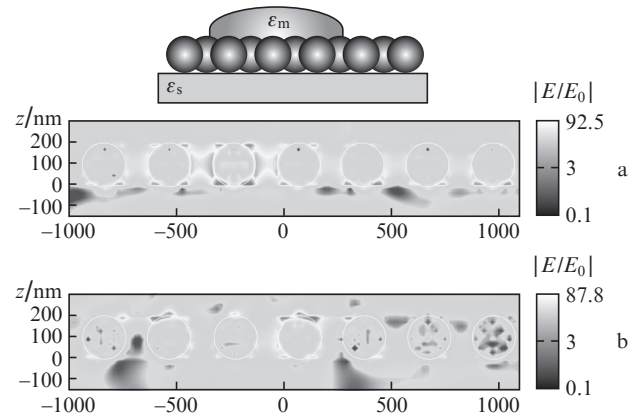


Figure 6. Near-field intensity distribution in the vicinity of an array of Au nanoparticles with a radius of 100 nm deposited on a dielectric substrate with a dielectric constant ϵ_s . On the top of the array is deposited a dielectric material with the dielectric constant ϵ_m . The distribution of the electric field intensity is shown for (a) $\epsilon_s > \epsilon_m = \epsilon_s/2$ and (b) $\epsilon_s < \epsilon_m = 2\epsilon_s$.

The ordered structures shown above are used to study the main dependences of the nanoparticle optical properties on different array characteristics. If no special conditions are taken into account, the nanoparticles deposited from colloids form structures of arbitrary shape. Figure 7 shows a TEM image of a slice of HeLa tumour cell with deposited gold nanoparticles 40 nm in diameter. The sample is prepared from the cell line (HeLa) cultured in a medium supplemented with 10% fetal bovine serum, 100 u mL^{-1} penicillin and 0.1 mg mL^{-1} streptomycin. Cells are maintained in a log growth phase at 37°C in a humidified air with 5% CO_2 . After incubation overnight the cells are mixed with gold nanoparticle colloid (BBInternational) with a particle diameter of 40 nm. More details on the sample preparation can be found in [23]. The nanoparticles shown in the inset Fig. 7 are arranged randomly and present a typical configuration observed when HeLa cells are mixed with nanoparticle colloids. Figure 7 presents the theoretical extinction, absorption and scattering spectra of this structure. It is seen that the maximal absorption for the array is at approximately 600 nm. The scattering efficiency maximum is red shifted and its magnitude is lower compared to the absorption one.

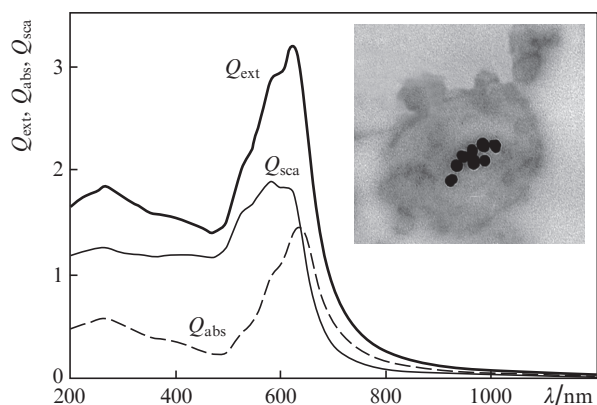


Figure 7. Calculated optical spectra of an ensemble of nanoparticles. The inset shows the TEM image of a slice of the HeLa tumour cell with deposited gold nanoparticles 40 nm in diameter.

4. Conclusions

Theoretical calculations of the optical properties of gold nanoparticle ensembles are performed on the basis of the generalised multiparticle Mie approach and FDTD technique. The far- and near-field properties show specific features that can be influenced more efficiently by the system characteristics compared to the case of a single particle. The absorption efficiency can be shifted to the IR spectrum range by increasing array size and decreasing interparticle distance. Elongated structures (for example, nanoparticle chain) demonstrate the most efficient shift of the absorption maximum to the IR region. With increasing array size the scattering dominates over the absorption as the scattering maximum is red shifted with respect to absorption one. For closely packed array the zones with the maximal field intensity are formed in the gaps between particles. In these hot spots the field intensity is enhanced by two orders of magnitude. The formation and characteristics of these zones depend on the dielectric properties of the environment. Such an analysis is shown for a complex system consisting of nanoparticle on a substrate and material on the top of the nanoparticles. The obtained results can be used in designing systems for applications in biophotonics such as photothermal therapy and bioimaging and in fabrications of SERS substrates.

Acknowledgements. The authors would like to acknowledge the financial support from the Bulgarian Science Fund (Contract No. DO 02-293).

References

- Ozbay E. *Science*, **311**, 189 (2006).
- Kreibig U., Vollmer M. (Eds) *Optical Properties of Metal Clusters* (Berlin: Springer, 1995).
- Noguez C. *J. Phys. Chem. C*, **111**, 3806 (2007).
- Sharma P., Brown S., Walter G., Santra S., Moudgli Br. *Adv. Coll. Interf. Sci.*, **123**, 471 (2006).
- Nedyalkov N.N., Atanasov P.A., Obara M. *Nanotechnol.*, **18**, 305703 (2007).
- Quinten M. *Optical Properties of Nanoparticle Systems. Mie and Beyond* (Weinheim: Wiley-VCH, 2011).
- Pissuwan D., Valenzuela S.M., Cortie M. *Trends Biotech.*, **24**, 62 (2006).
- Link S., Wang Z.L., El-Sayed M.A. *J. Phys. Chem. B*, **103**, 3529 (1999).
- Jain P.K., El-Sayed I.H., El-Sayed M.A. *Nanotoday*, **2**, 18 (2007).
- Kneipp K., Wang Y., Kneipp H., Perelman L.T., Itzkan I., Dasari R.R., Feld M.S. *Phys. Rev. Lett.*, **78**, 1667 (1997).

- Lin M., Chen H., Gwo Sh. *J. Am. Chem. Soc.*, **132**, 11259 (2010).
- Pinchuk A.O., Schatz G.C. *Mat. Sci. Eng. B*, **149**, 251 (2008).
- Hohenau A., Leitner A., Aussenegg F.R. *Springer Ser. Opt. Sci.*, **131**, 11 (2007).
- Zou S., Jarel N., Schatz G.C. *J. Chem. Phys.*, **120**, 10871 (2004).
- Khlebtsov B., Zharov V., Melnikov A., Tuchin V., Khlebtsov N. *Nanotechnol.*, **17**, 5167 (2006).
- www.astro.ufl.edu/~xu.
- Vo-Dinh T. *Biomedical Photonics Handbook* (New York: CRC Press, 2003).
- Taflove A., Hagness S.C. *Computational Electrodynamics: The Finite-Difference Time-Domain Method* (Boston: Artech House, 2000).
- Sendur K., Challener W., Peng C. *J. Appl. Phys.*, **96**, 2743 (2004).
- Johnson P.B., Christy R.W. *Phys. Rev. B*, **6**, 4370 (1972).
- Palik E.D. (Ed.) *Handbook of Optical Constants of Solids* (San Diego: Acad. Press, 1998).
- Leiderer P., Bartels C., König-Birk J., Mosbacher M., Boneberg J. *Appl. Phys. Lett.*, **85**, 5370 (2004).
- Nedyalkov N.N., Imamova S.E., Atanasov P.A., Toshkova R.A., Gardeva E.G., Yossifova L.S., Alexandrov M.T., Obara M. *Appl. Surf. Sci.*, **257**, 5456 (2011).